DALTON
FULL PAPER

Syntheses, crystal structures and magnetic properties of dinuclear copper(II) complexes with pyrazino[2,3-*f*][4,7]phenanthroline (pap) as bridging ligand

Hilde Grove,[a] Jorunn Sletten,[a] Miguel Julve[b] and Francesc Lloret[b]

[a] *Department of Chemistry, University of Bergen, Allégaten 41, N-5007 Bergen, Norway*
[b] *Department of Inorganic Chemistry, Faculty of Chemistry, University of Valencia, Dr. Moliner 50, 46100 Burjassot (Valencia), Spain*

Received 22nd September 1999, Accepted 22nd December 1999

Three dinuclear copper(II) complexes with pyrazino[2,3-*f*][4,7]phenanthroline (pap) as bridging ligand have been prepared; $[Cu_2(pap)(C_2O_4)_2]\cdot 5H_2O$ **1**, $[Cu_2(pap)(H_2O)_7(SO_4)]SO_4\cdot 3H_2O$ **2** and $[Cu_2(pap)(H_2O)_3(NO_3)_3]NO_3$ **3**. These are the first metal complexes of pap which have been characterized by X-ray crystallography and magnetic susceptibility measurements. In **1** the dinuclear complex is intercepted by a mirror plane; the bridging pap and the terminal oxalate ligands are bidentate in the equatorial plane of copper. In addition copper has weak axial interactions to oxygen atoms of oxalate in two neighbouring molecules. In **2** the two crystallograpically independent copper atoms are both six-co-ordinated with bridging pap and water molecules in equatorial positions, the axial positions being occupied by two water molecules or one water molecule and one sulfate oxygen atom, respectively. In **3** the co-ordination geometry of one copper is close to square pyramidal with pap, one nitrate oxygen atom and one water in equatorial positions; another water occupies the apical position. The description of the co-ordination sphere of the other copper is complicated by the presence of disorder in one of the co-ordinated nitrate groups. When considering only the major site of the disordered nitrate, the co-ordination geometry may in a first approximation be described as square pyramidal with a significant trigonal bipyramidal distortion. In the square pyramidal description the two pap nitrogen atoms, one water and one nitrate oxygen constitute the equatorial plane and a nitrate oxygen is situated in apical position. All the co-ordinated nitrate ions have a second weak Cu · · · O interaction. The Cu · · · Cu separations across bridging pap are 6.740 (**1**), 6.834 (**2**) and 6.808 Å (**3**). Variable-temperature susceptibility measurements reveal Curie law behaviour with very weak intramolecular antiferromagnetic coupling in all three compounds, the relevant parameters being $J = -1.4$ cm^{-1}, $g = 2.06$ for **1**, $J = -1.5$ cm^{-1}, $g = 2.10$ for **2**, and $J = -1.3$ cm^{-1}, $g = 2.08$ for **3** (the Hamiltonian being $H = -J\, S_A \cdot S_B$).

Introduction

The synthesis of pyrazino[2,3-*f*][4,7]phenanthroline, pap, was first published in 1957, and later a slightly modified procedure has been reported.[1] During the last decade studies on the electronic and photophysical properties of rhenium and ruthenium complexes of pap have appeared.[2] In particular studies of these and other polypyridine complexes have aimed at producing compounds with unusual excited state redox properties, and at utilizing these in fundamental investigations of electron- and energy-transfer processes. Also the interaction of pap–ruthenium complexes with DNA has been explored.[3] Otherwise the co-ordinating properties and metal complexes of this potentially very interesting heterocyclic, conjugated ligand do not appear to have been studied.

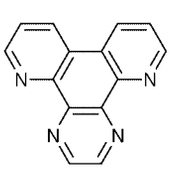
pap

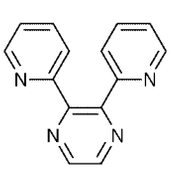
dpp

This compound may adopt both chelating and bis(chelating) co-ordination modes, and thus has the ability to form mononuclear as well as di- and poly-nuclear complexes. A variety of structural motifs are possible, and both chain and framework structures may result. A bridging pap ligand may be expected to propagate magnetic exchange between paramagnetic metal centers. It is well known that the related 2,2′-bipyrimidine ligand very efficiently transmits a strong antiferromagnetic interaction through the σ pathway.[4] In the majority of pyrazine complexes studied so far the magnetic interaction is weak and of antiferromagnetic character, and there has been a debate on whether the exchange takes place through a σ or a π pathway.[5] Recently, relatively strong antiferromagnetic interaction has been discovered in copper(II) and nickel(II) complexes of 2,3,5,6-tetra(2-pyridyl)pyrazine,[6] the co-ordination geometries being such that the σ pathway is favoured. Some of us have studied copper(II) complexes of 2,3-di-2-pyridylpyrazine, dpp, where steric hindrance causes a non-planar arrangement both in the ligand itself and in its metal complexes, and often gives irregular metal co-ordination geometries. In the dpp-bridged complexes obtained up to this point the copper co-ordination and ligand geometries have not been optimal for transmitting magnetic interaction, neither through the σ nor the π pathway.[7] However, with the planar pap bridging ligand this situation might be expected to change; dinuclear complexes with bridging pap co-ordinating equatorially to octahedral, square pyramidal or square planar copper(II) are likely to be obtained, and would reveal whether the σ pathway is effective through this heterocyclic system.

With the intention of investigating the co-ordinating properties of pap and the possible ability of this ligand to propagate magnetic exchange through the σ pathway, we have prepared three dinuclear copper(II) complexes with pap as bridging ligand; $[Cu_2(pap)(C_2O_4)_2]\cdot 5H_2O$ **1**, $[Cu_2(pap)(H_2O)_7(SO_4)]SO_4\cdot 3H_2O$ **2** and $[Cu_2(pap)(H_2O)_3(NO_3)_3]NO_3$ **3**. Their syntheses, crystal structures and magnetic properties are presented herein. To our knowledge no structure determinations or magnetic

DOI: 10.1039/a907658a

characterization of metal complexes of pap have been reported previously. Further work aimed at producing polynuclear network compounds utilizing pap as bridging ligand is in progress.

Experimental

Materials

Pyrazino[2,3-*f*][4,7]phenanthroline (pap) was prepared from 4,7-phenanthroline-5,6-dione (a generous gift from Novartis Norge AS) by the procedure of Schmidt and Druey.[1a] All other chemicals were purchased from commercial sources and used as received.

Preparations

$[Cu_2(pap)(C_2O_4)_2]\cdot 5H_2O$ 1. This complex was prepared by adding 0.015 mmol (3.4 mg) of pap and 0.029 mmol (7.0 mg) of $Cu(NO_3)_2\cdot 3H_2O$ dissolved in 4 mL of water to an aqueous solution (6 mL) containing 0.029 mmol (3.9 mg) of $Na_2C_2O_4$. Slow evaporation at room temperature gave dark green, plate formed crystals suitable for X-ray diffraction work. The crystals disintegrate in air in the course of a few hours (Found: C, 34.9; H, 3.0; N, 9.1; O, 32.7. Calc. for $C_{18}H_{18}Cu_2N_4O_{13}$: C, 34.6; H, 2.9; N, 9.0; O, 33.3%). Oxygen analysis by iodometric method.[8]

$[Cu_2(pap)(H_2O)_7(SO_4)]SO_4\cdot 3H_2O$ 2. Aqueous solutions (3 mL each one) containing 0.029 mmol (7.2 mg) of $CuSO_4\cdot 5H_2O$ and 0.014 mmol (3.3 mg) of pap, respectively, were mixed. Slow evaporation at room temperature of the resulting green solution afforded light green crystals suitable for X-ray diffraction. The crystals disintegrate slowly in air at room temperature in the course of a few days (Found: C, 24.0; H, 3.7; N, 8.1; O, 36.6. Calc. for $C_7H_{14}CuN_2O_9S$: C, 23.0; H, 3.9; N, 7.7; O, 39.4. Calc. on the assumption of loss of on average two molecules of crystal water per dinuclear unit in the disintegration: C, 24.2; H, 3.5; N, 8.1; O, 36.8%). Oxygen analysis by iodometric method.[8]

$[Cu_2(pap)(H_2O)_3(NO_3)_3]NO_3$ 3. Aqueous solutions (5 mL each one) containing 0.061 mmol (14.7 mg) of $Cu(NO_3)_2\cdot 3H_2O$ and 0.031 mmol (7.1 mg) of pap, respectively, were mixed. Partial evaporation followed by addition of Pr^iOH gave a microcrystalline product, used for the susceptibility measurements. Evaporation at room temperature to almost dryness gave green crystalline plates suitable for X-ray diffraction. The crystals are stable in air over several months. (Found: C, 25.2; H, 2.2; N, 16.1. Calc. for $C_{14}H_{14}Cu_2N_8O_{15}$: C, 25.5; H, 2.1; N, 16.9%).

Physical techniques

Infrared spectra were recorded with a Nicolet 800 FTIR spectrophotometer as KBr pellets in the 4000–400 cm^{-1} region. The magnetic susceptibility measurements of polycrystalline samples were measured over the temperature range 2.0–290 K with a Quantum Design SQUID susceptometer and using an applied magnetic field of 0.1 T. The complex $(NH_4)_2Mn(SO_4)_2\cdot 6H_2O$ was used as a susceptibility standard. Diamagnetic corrections of the constituent atoms were estimated from Pascal's constants and found to be -285×10^{-6} (**1** and **3**) and -380×10^{-6} cm^3 mol^{-1} (**2**).[9] A value of 60×10^{-6} cm^3 mol^{-1} was used for the temperature-independent paramagnetism of the copper(II) ion.

The ESR spectra on polycrystalline samples of compounds **1**–**3** were recorded on a Bruker ESP350 spectrometer, equipped with a standard Oxford low-temperature device operating at X-band. The magnetic field was measured with a Bruker BNM 200 gaussimeter and the frequency determined by using a Hewlett-Packard 5352B microwave frequency counter.

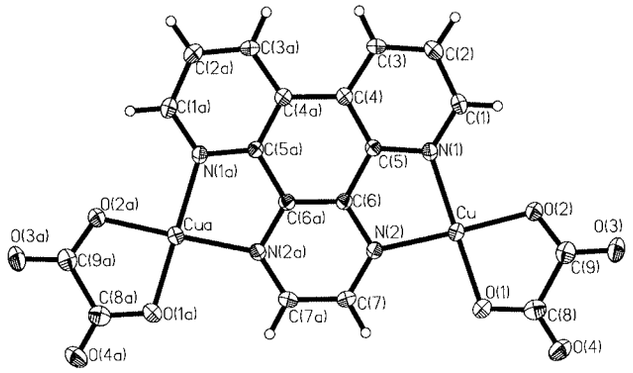

Fig. 1 Dinuclear complex unit in $[Cu_2(pap)(C_2O_4)_2]\cdot 5H_2O$ **1**. Thermal ellipsoids are plotted at the 50% probability level. Symmetry operation (a) = $x, -y, z$.

Crystallography

Diffraction data of all three compounds were collected at 173 K with a 2K SMART CCD area detector diffractometer using ω rotation scans with a scan width of 0.3°, and graphite-monochromated Mo-Kα radiation (λ 0.71073 Å). Owing to disintegration in air the crystal of **1** was sealed and mounted in paratone-n oil. The data collection covered a hemisphere of reciprocal space in the case of **1** and the full spheres for **2** and **3** (2θ 54, 60 and 61° for **1**, **2** and **3**, respectively). Empirical absorption corrections were carried out (SADABS).[10] In the case of compound **3** the space group is uniquely determined by the systematic extinctions ($P2_1/n$), whereas for **1** and **2** the centrosymmetric space groups $C2/m$ and $P\bar{1}$ were chosen based on intensity statistics, and proved to be correct through the successful refinements of the structures. The structures were solved by the Patterson method and refined by full-matrix least squares based on F^2 and including all reflections. In compound **3** one of the co-ordinated nitrate ions is disordered; the major and minor sites of the individual oxygen atoms were refined, occupancy factors were adjusted and in the final cycles of refinement fixed at their average values of 0.80 and 0.20, respectively. All non-hydrogen atoms were anisotropically refined. Hydrogen atoms bound to carbon were included at idealized, calculated positions while those bound to oxygen (except those belonging to one water molecule with rather high thermal displacement parameters in compound **1**) were located in Fourier-difference maps. For compounds **1** and **2** positional and thermal parameters of all hydrogen atoms were adjusted according to the riding model. In **3** isotropic refinement of water hydrogen atoms was performed because the electron distribution in the region of a relatively strong hydrogen bond, O(1)···O(15) 2.640(3) Å, indicated the presence of an elongated O–H bond. Refinement of hydrogen positions resulted in an O(1)–H bond length of 1.26(3) Å. The same feature was also observed in a second structure determination of this compound with data collected at room temperature on another crystal from a different preparation, and thus appears to be consistent. Crystal parameters and refinement results are summarized in Table 1.

For data collections and data integration the SMART and SAINT programs were used.[11] Structure solutions, refinements and graphics were performed with the SHELXS 86, SHELXL 93 and XP programs.[12] Selected bond distances and angles are listed in Tables 2–4.

CCDC reference number 186/1789.

See http://www.rsc.org/suppdata/dt/a9/a907658a/ for crystallographic files in .cif format.

Results and discussion

Structures

$[Cu_2(pap)(C_2O_4)_2]\cdot 5H_2O$ 1. The structure is built of neutral, dinuclear $Cu_2(pap)(C_2O_4)_2$ units (Fig. 1) and water molecules of

Table 1 Summary of crystallographic data and structure refinement for $[Cu_2(pap)(C_2O_4)_2]\cdot 5H_2O$ **1**, $[Cu_2(pap)(H_2O)_7(SO_4)]SO_4\cdot 3H_2O$ **2** and $[Cu_2(pap)(H_2O)_3(NO_3)_3]NO_3$ **3**

	1	**2**	**3**
Formula	$C_{18}H_{18}Cu_2N_4O_{13}$	$C_{14}H_{28}Cu_2N_4O_{18}S_2$	$C_{14}H_{14}Cu_2N_8O_{15}$
M	625.44	731.60	661.41
Crystal system	Monoclinic	Triclinic	Monoclinic
Space group	$C2/m$	$P\bar{1}$	$P2_1/n$
a/Å	18.3692(11)	7.3457(2)	8.7332(3)
b/Å	17.6964(7)	13.2214(4)	9.0065(3)
c/Å	7.0048(4)	14.5128(3)	27.6888(4)
α/°		114.229(1)	
β/°	102.902(2)	99.134(1)	98.149(2)
γ/°		90.252(1)	
U/Å^3	2219.6(2)	1265.24(6)	2155.89(11)
Z	4	2	4
D_c/g cm^{-3}	1.872	1.920	2.038
μ/mm^{-1}	1.997	1.939	2.073
Reflections collected	10296	20876	36387
Unique reflections	2505 (R_{int} = 0.037)	7371 (R_{int} = 0.028)	6554 (R_{int} = 0.054)
R [$I > 2\sigma(I)$]	0.0403	0.0293	0.0347
R_w [$I > 2\sigma(I)$]	0.1082	0.0682	0.703

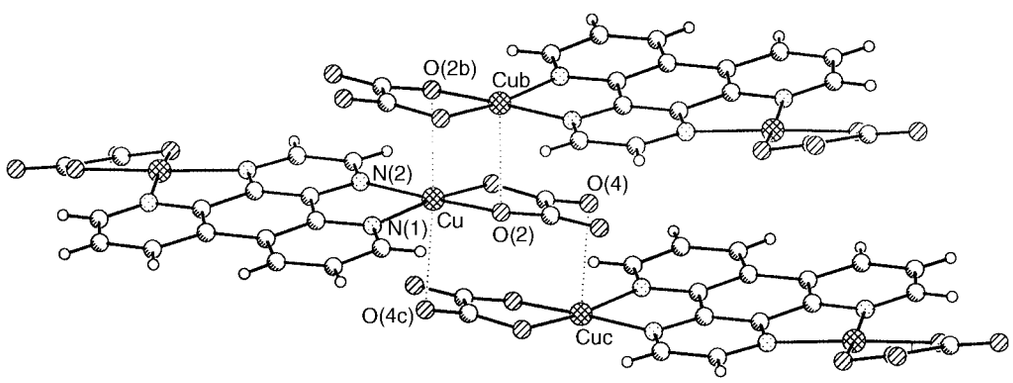

Fig. 2 Stacks of $[Cu_2(pap)(C_2O_4)_2]$ units along the crystallographic c axis. The weak axial Cu–O interactions are shown as dotted lines; Cu–O(2b) 2.631(3), Cu–O(4c) 2.612(3) Å; (b) 0.5 − x, 0.5 − y, −z, (c) 0.5 − x, 0.5 − y, 1 − z.

hydration. A crystallographic mirror plane cuts the dinuclear unit through the midpoints of the C(4)–C(4a), C(6)–C(6a), C(7)–C(7a) bonds. The bridging pap ligand and the terminal oxalate are both bidentate in the equatorial plane of copper [Cu–$N_{phenanthroline}$ 1.998(3), Cu–$N_{pyrazine}$ 2.011(3) and Cu–O 1.934(2) and 1.938(2) Å]. In addition copper has weak axial interactions to oxygen atoms of oxalate in two neighbouring molecules [Cu–O 2.612(3) and 2.631(3) Å]. This semi-co-ordination[13a] links the molecular units into chains of parallel stacked molecules (Fig. 2), the stacks running along the crystallographic c axis. One of the water molecules (O(6)) forms bifurcated hydrogen bonds to the non-co-ordinated oxalate oxygen atoms of two complex units related by a mirror plane, thus linking molecules along the b axis. The same water molecule also has short O···H–C(3,3a) contacts [O···H being 2.37 and 2.46 Å] to another neighbouring molecule; these interactions link molecules into sheets running normal to the stacks described above. The other water molecules provide hydrogen bonds crosslinking sheets and stacks.

The copper equatorial plane has a small tetrahedral distortion [atomic deviations 0.084–0.088 Å] with copper being slightly displaced by 0.038 Å from the mean plane; the two symmetry related equatorial planes are tilted 2.8° relative to one another. The pap and C_2O_4 ligands are both almost planar and make dihedral angles of 5.1 and 13.7°, respectively, with the copper equatorial plane; copper deviates by 0.055 Å from the pap mean plane. The angles between the pap and C_2O_4 planes, and between the planes of the two terminal C_2O_4 groups, are 18.5 and 19.9°, respectively. The Cu···Cu separation across the pap bridge is 6.740 Å; the metal–metal separations within the chain of stacked molecules are Cu···Cub 3.437 Å [(b) 0.5 − x, 0.5 − y, −z] and Cu···Cuc 4.931 Å [(c) 0.5 − x, 0.5 − y, 1 − z].

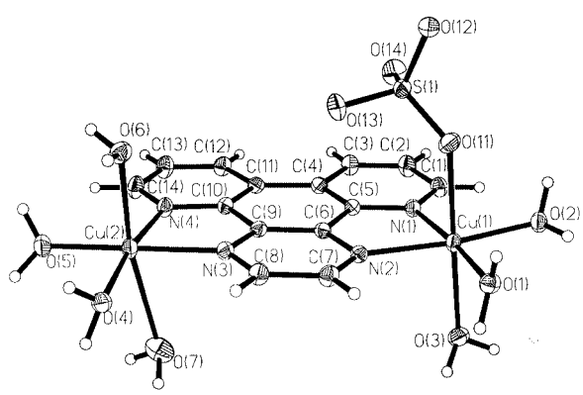

Fig. 3 Dinuclear complex unit in $[Cu_2(pap)(H_2O)_7(SO_4)]SO_4\cdot 3H_2O$ **2**. Thermal ellipsoids are plotted at the 50% probability level.

$[Cu_2(pap)(H_2O)_7(SO_4)]SO_4\cdot 3H_2O$ 2. The structure consists of $[Cu_2(pap)(H_2O)_7(SO_4)]^{2+}$ dinuclear complex units (Fig. 3), unco-ordinated sulfate counter ions and water of crystallization. The two copper atoms are crystallographically independent, both metal atoms are six-co-ordinated with the bridging pap ligand and water molecules in equatorial positions [Cu–$N_{phenanthroline}$ 2.035(2) and 2.032(2), Cu–$N_{pyrazine}$ 2.055(2) and 2.054(2), Cu–O from 1.974(1) to 1.994(1) Å], the axial positions being occupied by two water molecules [Cu(2)–O 2.277(1) and 2.442(2) Å] or one water molecule and one sulfate oxygen atom [Cu(1)–O_{water} 2.285(1), Cu(1)–$O_{sulfate}$ 2.283(1) Å].

The equatorial planes of both copper atoms have slight tetrahedral distortions, the maximum atomic deviations from the mean equatorial planes of Cu(1) and Cu(2) being 0.043 and 0.028 Å, respectively. The metal atoms are displaced by 0.024 and 0.076 Å out of the mean planes towards axial water O(3) and O(6), respectively. The pap ligand is almost planar and makes dihedral angles of 4.5 and 6.5° with the equatorial planes of Cu(1) and Cu(2), the two metal atoms deviating 0.044 and 0.082 Å from the pap mean plane. The Cu···Cu separation across the pap bridge is 6.834 Å. The shortest intermolecular metal–metal distances are Cu(1)···Cu(1a) 5.640 [(a) $-x$, $2-y$, $1-z$], Cu(1)···Cu(1i) 6.289 [(i) $1-x$, $2-y$, $1-z$] and Cu(2)···Cu(1b) 6.558 Å [(b) x, $y-1$, z]. The shortest of these occurs between molecules connected by hydrogen bonding through co-ordinated water of the reference molecule and co-ordinated sulfate in molecule (a). All sulfate oxygen atoms, except the one co-ordinated to Cu(1), and all water molecules participate in hydrogen bonding and link the molecules in an elaborate three dimensional network.

The unco-ordinated sulfate ion is close to regular tetrahedral with S–O bond lengths and O–S–O bond angles in the ranges 1.477(1) to 1.489(1) Å and 108.80(8) to 110.24(9)°, respectively. The co-ordinated sulfate deviates slightly more from tetrahedral symmetry, bond lengths and angles being in the ranges 1.463(1) to 1.505(1) Å and 107.69(8) to 111.75(9)°, respectively.

$[Cu_2(pap)(H_2O)_3(NO_3)_3]NO_3$ 3. The structure consists of dinuclear $[Cu_2(pap)(H_2O)_3(NO_3)_3]^+$ complex units (Fig. 4) and nitrate counter ions. The co-ordination geometry of Cu(1) is close to square pyramidal with pap, one nitrate oxygen atom and one water in equatorial positions [Cu–$N_{phenanthroline}$ 2.018(2), Cu–$N_{pyrazine}$ 2.037(2), Cu–O(4) 1.977(2), Cu–O(2) 1.980(2) Å]; another water occupies the apical position [Cu–O(1) 2.278(2) Å]. The other copper, Cu(2), is surrounded by pap, a water molecule and two nitrate ions, one of the latter ions is disordered, the occupancy of the major and minor sites being 0.80 and 0.20, respectively. When considering only the major site of the disordered nitrate, the Cu(2) co-ordination geometry may in a first approach be described as square pyramidal with a significant trigonal bipyramidal distortion (Fig. 5a). In the square pyramidal description the two pap nitrogen atoms [Cu–$N_{phenanthroline}$ 1.992(2), Cu–$N_{pyrazine}$ 2.062(2) Å], one

Table 2 Selected bond lengths (Å) and angles (°) for $[Cu_2(pap)(C_2O_4)_2]\cdot 5H_2O$ **1** with e.s.d.s in parentheses

Copper co-ordination sphere			
Cu–O(1)	1.934(2)	Cu–N(2)	2.011(3)
Cu–O(2)	1.938(2)	Cu–O(4c)	2.612(3)
Cu–N(1)	1.998(3)	Cu–O(2b)	2.631(3)
O(1)–Cu–O(2)	85.52(10)	N(1)–Cu–O(4c)	85.58(9)
O(1)–Cu–N(1)	172.79(11)	N(2)–Cu–O(4c)	85.17(9)
O(2)–Cu–N(1)	94.37(10)	O(1)–Cu–O(2b)	98.88(9)
O(1)–Cu–N(2)	96.74(10)	O(2)–Cu–O(2b)	83.59(10)
O(2)–Cu–N(2)	176.51(10)	N(1)–Cu–O(2b)	88.26(9)
N(1)–Cu–N(2)	83.72(11)	N(2)–Cu–O(2b)	93.41(9)
O(1)–Cu–O(4c)	87.29(9)	O(4c)–Cu–O(2b)	173.79(8)
O(2)–Cu–O(4c)	97.62(10)		
pap bridging ligand			
N(1)–C(1)	1.330(4)	C(3)–C(4)	1.398(4)
N(1)–C(5)	1.353(4)	C(4)–C(5)	1.402(4)
N(2)–C(7)	1.336(4)	C(4)–C(4a)	1.469(6)
N(2)–C(6)	1.363(4)	C(5)–C(6)	1.443(4)
C(1)–C(2)	1.400(5)	C(6)–C(6a)	1.375(6)
C(2)–C(3)	1.371(5)	C(7)–C(7a)	1.398(7)
C(1)–N(1)–C(5)	118.6(3)	C(3)–C(4)–C(4a)	124.1(2)
C(1)–N(1)–Cu	129.2(2)	C(5)–C(4)–C(4a)	118.8(2)
C(5)–N(1)–Cu	112.2(2)	N(1)–C(5)–C(4)	123.2(3)
C(7)–N(2)–C(6)	116.8(3)	N(1)–C(5)–C(6)	115.7(3)
C(7)–N(2)–Cu	133.1(2)	C(4)–C(5)–C(6)	121.1(3)
C(6)–N(2)–Cu	110.0(2)	N(2)–C(6)–C(6a)	121.5(2)
N(1)–C(1)–C(2)	121.6(3)	N(2)–C(6)–C(5)	118.3(3)
C(3)–C(2)–C(1)	120.0(3)	C(6a)–C(6)–C(5)	120.1(2)
C(2)–C(3)–C(4)	119.5(3)	N(2)–C(7)–C(7a)	121.7(2)
C(3)–C(4)–C(5)	117.1(3)		

Symmetry transformations used to generate equivalent atoms: (a) x, $-y$, z; (b) $-x+\frac{1}{2}$, $-y+\frac{1}{2}$, $-z$; (c) $-x+\frac{1}{2}$, $-y+\frac{1}{2}$, $-z+1$.

Table 3 Selected bond lengths (Å) and angles (°) for $[Cu_2(pap)(H_2O)_7(SO_4)]SO_4\cdot 3H_2O$ **2** with e.s.d.s in parentheses

Copper co-ordination spheres							
Cu(1)–O(1)	1.9834(13)	Cu(1)–N(2)	2.055(2)	Cu(2)–O(4)	1.9737(13)	Cu(2)–N(3)	2.054(2)
Cu(1)–O(2)	1.9912(13)	Cu(1)–O(11)	2.2827(14)	Cu(2)–O(5)	1.9942(14)	Cu(2)–O(6)	2.2769(14)
Cu(1)–N(1)	2.035(2)	Cu(1)–O(3)	2.2847(14)	Cu(2)–N(4)	2.032(2)	Cu(2)–O(7)	2.442(2)
O(1)–Cu(1)–O(2)	91.95(5)	N(1)–Cu(1)–O(11)	93.15(6)	O(4)–Cu(2)–O(5)	92.35(6)	N(4)–Cu(2)–O(6)	96.82(6)
O(1)–Cu(1)–N(1)	175.20(6)	N(2)–Cu(1)–O(11)	86.01(6)	O(4)–Cu(2)–N(4)	172.03(6)	N(3)–Cu(2)–O(6)	87.51(6)
O(2)–Cu(1)–N(1)	92.78(6)	O(1)–Cu(1)–O(3)	91.04(5)	O(5)–Cu(2)–N(4)	92.87(6)	O(4)–Cu(2)–O(7)	84.85(5)
O(1)–Cu(1)–N(2)	93.75(6)	O(2)–Cu(1)–O(3)	89.34(5)	O(4)–Cu(2)–N(3)	92.65(6)	O(5)–Cu(2)–O(7)	97.69(6)
O(2)–Cu(1)–N(2)	173.21(6)	N(1)–Cu(1)–O(3)	88.19(6)	O(5)–Cu(2)–N(3)	174.16(6)	N(4)–Cu(2)–O(7)	88.48(6)
N(1)–Cu(1)–N(2)	81.58(6)	N(2)–Cu(1)–O(3)	94.24(5)	N(4)–Cu(2)–N(3)	81.84(6)	N(3)–Cu(2)–O(7)	79.78(6)
O(1)–Cu(1)–O(11)	87.63(5)	O(11)–Cu(1)–O(3)	178.66(5)	O(4)–Cu(2)–O(6)	88.66(5)	O(6)–Cu(2)–O(7)	165.41(6)
O(2)–Cu(1)–O(11)	90.54(5)			O(5)–Cu(2)–O(6)	95.61(6)		
pap bridging ligand							
N(1)–C(1)	1.334(2)	N(4)–C(14)	1.336(2)	C(4)–C(5)	1.403(2)	C(9)–C(10)	1.448(2)
N(1)–C(5)	1.359(2)	N(4)–C(10)	1.358(2)	C(4)–C(11)	1.469(2)	C(10)–C(11)	1.405(2)
N(2)–C(7)	1.330(2)	C(1)–C(2)	1.403(3)	C(5)–C(6)	1.447(2)	C(11)–C(12)	1.414(2)
N(2)–C(6)	1.353(2)	C(2)–C(3)	1.377(3)	C(6)–C(9)	1.387(2)	C(12)–C(13)	1.383(3)
N(3)–C(8)	1.326(2)	C(3)–C(4)	1.411(2)	C(7)–C(8)	1.409(3)	C(13)–C(14)	1.402(3)
N(3)–C(9)	1.353(2)						
C(1)–N(1)–C(5)	118.0(2)	C(14)–N(4)–Cu(2)	128.91(13)	N(1)–C(5)–C(6)	115.3(2)	N(4)–C(10)–C(11)	124.1(2)
C(1)–N(1)–Cu(1)	128.62(13)	C(10)–N(4)–Cu(2)	113.00(12)	C(4)–C(5)–C(6)	120.4(2)	N(4)–C(10)–C(9)	115.5(2)
C(5)–N(1)–Cu(1)	113.36(11)	N(1)–C(1)–C(2)	121.7(2)	N(2)–C(6)–C(9)	121.4(2)	C(11)–C(10)–C(9)	120.3(2)
C(7)–N(2)–C(6)	117.1(2)	C(3)–C(2)–C(1)	120.4(2)	N(2)–C(6)–C(5)	118.4(2)	C(10)–C(11)–C(12)	116.6(2)
C(7)–N(2)–Cu(1)	131.32(13)	C(2)–C(3)–C(4)	119.2(2)	C(9)–C(6)–C(5)	120.1(2)	C(10)–C(11)–C(4)	119.2(2)
C(6)–N(2)–Cu(1)	111.25(11)	C(5)–C(4)–C(3)	116.5(2)	N(2)–C(7)–C(8)	121.5(2)	C(12)–C(11)–C(4)	124.2(2)
C(8)–N(3)–C(9)	117.3(2)	C(5)–C(4)–C(11)	119.5(2)	N(3)–C(8)–C(7)	121.4(2)	C(13)–C(12)–C(11)	119.3(2)
C(8)–N(3)–Cu(2)	131.60(12)	C(3)–C(4)–C(11)	124.0(2)	N(3)–C(9)–C(6)	121.3(2)	C(12)–C(13)–C(14)	119.9(2)
C(9)–N(3)–Cu(2)	110.97(12)	N(1)–C(5)–C(4)	124.3(2)	N(3)–C(9)–C(10)	118.3(2)	N(4)–C(14)–C(13)	122.1(2)
C(14)–N(4)–C(10)	118.0(2)			C(6)–C(9)–C(10)	120.4(2)		

Table 4 Selected bond lengths (Å) and bond angles (°) for $[Cu_2(pap)(H_2O)_3(NO_3)_3]NO_3$ **3** with e.s.d.s in parentheses. In the co-ordination sphere of copper semi-co-ordinated atoms as well as major and minor sites of nitrate are included

Copper co-ordination spheres							
Cu(1)–O(4)	1.977(2)	Cu(1)–N(2)	2.037(2)	Cu(2)–O(3)	1.944(2)	Cu(2)–O(8)	2.664(3)
Cu(1)–O(2)	1.980(2)	Cu(1)–O(1)	2.278(2)	Cu(2)–N(4)	1.992(2)	Cu(2)–O(11)	2.969(2)
Cu(1)–N(1)	2.018(2)	Cu(1)–O(5)	2.713(2)	Cu(2)–O(7)	2.055(5)	Cu(2)–O(81)	2.115(11)
				Cu(2)–N(3)	2.062(2)	Cu(2)–O(71)	2.46(2)
				Cu(2)–O(10)	2.179(2)		
O(4)–Cu(1)–O(2)	89.60(8)	N(1)–Cu(1)–O(1)	101.67(7)	O(3)–Cu(2)–N(4)	172.27(8)	N(3)–Cu(2)–O(71)	161.2(7)
O(4)–Cu(1)–N(1)	96.95(7)	N(2)–Cu(1)–O(1)	95.46(7)	O(3)–Cu(2)–O(7)	94.3(2)	O(81)–Cu(2)–O(71)	55.7(8)
O(2)–Cu(1)–N(1)	167.93(3)	O(4)–Cu(1)–O(5)	52.28(6)	N(4)–Cu(2)–O(7)	92.8(2)	O(10)–Cu(2)–O(71)	79.5(7)
O(4)–Cu(1)–N(2)	178.77(7)	O(2)–Cu(1)–O(5)	85.69(8)	O(3)–Cu(2)–N(3)	90.05(7)	O(3)–Cu(2)–O(8)	96.62(10)
O(2)–Cu(1)–N(2)	91.51(8)	N(1)–Cu(1)–O(5)	90.30(7)	N(4)–Cu(2)–N(3)	82.23(7)	N(4)–Cu(2)–O(8)	85.26(10)
N(1)–Cu(1)–N(2)	82.05(7)	N(2)–Cu(1)–O(5)	128.34(6)	O(7)–Cu(2)–N(3)	158.1(2)	O(7)–Cu(2)–O(8)	52.7(2)
O(4)–Cu(1)–O(1)	84.03(7)	O(1)–Cu(1)–O(5)	135.95(7)	O(3)–Cu(2)–O(81)	90.8(4)	N(3)–Cu(2)–O(8)	105.41(9)
O(2)–Cu(1)–O(1)	89.05(9)			N(4)–Cu(2)–O(81)	91.1(4)	O(10)–Cu(2)–O(8)	135.35(9)
				N(3)–Cu(2)–O(81)	105.9(4)	O(3)–Cu(2)–O(11)	106.53(7)
				O(3)–Cu(2)–O(10)	84.94(7)	N(4)–Cu(2)–O(11)	72.16(6)
				N(4)–Cu(2)–O(10)	99.03(7)	O(7)–Cu(2)–O(11)	121.2(2)
				O(7)–Cu(2)–O(10)	82.6(2)	N(3)–Cu(2)–O(11)	77.76(6)
				N(3)–Cu(2)–O(10)	119.22(6)	O(81)–Cu(2)–O(11)	162.4(4)
				O(81)–Cu(2)–O(10)	134.6(4)	O(10)–Cu(2)–O(11)	46.89(5)
				O(3)–Cu(2)–O(71)	93.7(7)	O(71)–Cu(2)–O(11)	118.5(7)
				N(4)–Cu(2)–O(71)	93.5(7)	O(8)–Cu(2)–O(11)	156.69(9)
pap bridging ligand							
N(1)–C(1)	1.339(3)	N(4)–C(14)	1.334(3)	C(4)–C(5)	1.402(3)	C(9)–C(10)	1.438(3)
N(1)–C(5)	1.361(3)	N(4)–C(10)	1.363(3)	C(4)–C(11)	1.469(3)	C(10)–C(11)	1.404(3)
N(2)–C(7)	1.326(3)	C(1)–C(2)	1.404(3)	C(5)–C(6)	1.443(3)	C(11)–C(12)	1.412(3)
N(2)–C(6)	1.358(3)	C(2)–C(3)	1.380(3)	C(6)–C(9)	1.380(3)	C(12)–C(13)	1.375(3)
N(3)–C(8)	1.324(3)	C(3)–C(4)	1.408(3)	C(7)–C(8)	1.415(3)	C(13)–C(14)	1.395(3)
N(3)–C(9)	1.361(3)						
C(1)–N(1)–C(5)	117.9(2)	C(14)–N(4)–Cu(2)	127.8(2)	N(1)–C(5)–C(6)	115.1(2)	N(4)–C(10)–C(11)	123.8(2)
C(1)–N(1)–Cu(1)	128.6(2)	C(10)–N(4)–Cu(2)	113.86(14)	C(4)–C(5)–C(6)	120.5(2)	N(4)–C(10)–C(9)	115.5(2)
C(5)–N(1)–Cu(1)	113.30(14)	N(1)–C(1)–C(2)	121.7(2)	N(2)–C(6)–C(9)	121.5(2)	C(11)–C(10)–C(9)	120.7(2)
C(7)–N(2)–C(6)	117.0(2)	C(3)–C(2)–C(1)	120.2(2)	N(2)–C(6)–C(5)	118.2(2)	C(10)–C(11)–C(12)	116.4(2)
C(7)–N(2)–Cu(1)	131.4(2)	C(2)–C(3)–C(4)	119.5(2)	C(9)–C(6)–C(5)	120.2(2)	C(10)–C(11)–C(4)	118.9(2)
C(6)–N(2)–Cu(1)	111.05(13)	C(5)–C(4)–C(3)	116.4(2)	N(2)–C(7)–C(8)	121.7(2)	C(12)–C(11)–C(4)	124.7(2)
C(8)–N(3)–C(9)	117.2(2)	C(5)–C(4)–C(11)	119.2(2)	N(3)–C(8)–C(7)	121.3(2)	C(13)–C(12)–C(11)	119.4(2)
C(8)–N(3)–Cu(2)	132.4(2)	C(3)–C(4)–C(11)	124.3(2)	N(3)–C(9)–C(6)	121.4(2)	C(12)–C(13)–C(14)	120.6(2)
C(9)–N(3)–Cu(2)	110.28(14)	N(1)–C(5)–C(4)	124.4(2)	N(3)–C(9)–C(10)	118.1(2)	N(4)–C(14)–C(13)	121.5(2)
C(14)–N(4)–C(10)	118.4(2)			C(6)–C(9)–C(10)	120.4(2)		

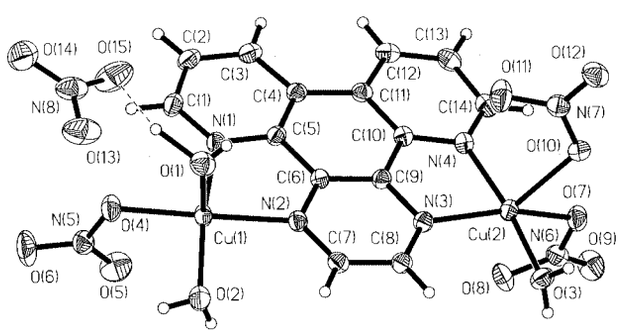

Fig. 4 Formula unit of $[Cu_2(pap)(H_2O)_3(NO_3)_3]NO_3$ **3**. Thermal ellipsoids are plotted at the 50% probability level. Only the major site of the disordered co-ordinated nitrate [N(6)] is included. The hydrogen bond linking the counter ion to the co-ordination sphere of Cu(1) is indicated by a dashed line.

water [Cu–O(3) 1.944(2) Å] and one nitrate oxygen [Cu–O(7) 2.055(5) Å] constitute the equatorial plane and a nitrate oxygen atom is situated in apical position [Cu–O(10) 2.179(2) Å]. In the trigonal bipyramidal description a pap pyrazine nitrogen and oxygen atoms, O(7) and O(10), from two nitrate ions form the equatorial plane, while pap pyridine nitrogen and water are in axial positions. When considering the minor nitrate site the co-ordination geometry for Cu(2) is best described by the distorted trigonal bipyramidal model, the nitrate oxygen atoms now co-ordinating equatorially being O(81) and O(10) (Fig. 5b). The τ value, commonly used to describe the degree of trigonal distortion,[14] attains the value 0.18 for Cu(1), while it is 0.24 and 0.63 for Cu(2) bound to major site and minor site nitrate, respectively. The τ parameter only takes into account bond angles, but when comparing the bond distances in the co-ordination spheres of the two copper atoms the more pronounced trigonal distortion of Cu(2), also for the major site nitrate, is quite evident. The equatorial plane of Cu(1) has a moderate tetrahedral distortion (maximum atomic deviation 0.098 Å) and copper is displaced by 0.083 Å from the mean plane towards the apical ligand. The square pyramidal description of the Cu(2) co-ordination sphere reveals a much more pronounced tetrahedral distortion with maximum atomic deviation being 0.188 Å and the copper atom displaced by 0.206 Å towards the axial O(10). In the above description of the co-ordination geometries the nitrate ions have been considered monodentate. However, they are oriented such that in each one of the other oxygen atoms makes an additional contact to copper [Cu(1)–O(5) 2.713(2), Cu(2)–O(8) 2.664(3) (major site nitrate), Cu(2)–O(71) 2.460(19) Å (minor site nitrate), Cu(2)–O(11) 2.969(2) Å]. The unsymmetrical bidentate co-ordination mode of nitrate is well known;[15] the three shorter of the above listed contacts clearly fall within the range referred to as semi-co-ordination,[13a] while the fourth is a limiting case. If the three shorter of these contacts are taken into account the co-ordination spheres may be described as strongly distorted octahedral 4 + 1 + 1*.[13b] The copper equatorial planes [based on the square pyramidal descriptions for both Cu(1) and Cu(2)] make angles of 11.5 and 13.5°, respectively, with the mean plane of the pap ligand, the copper atoms deviating by 0.225 and

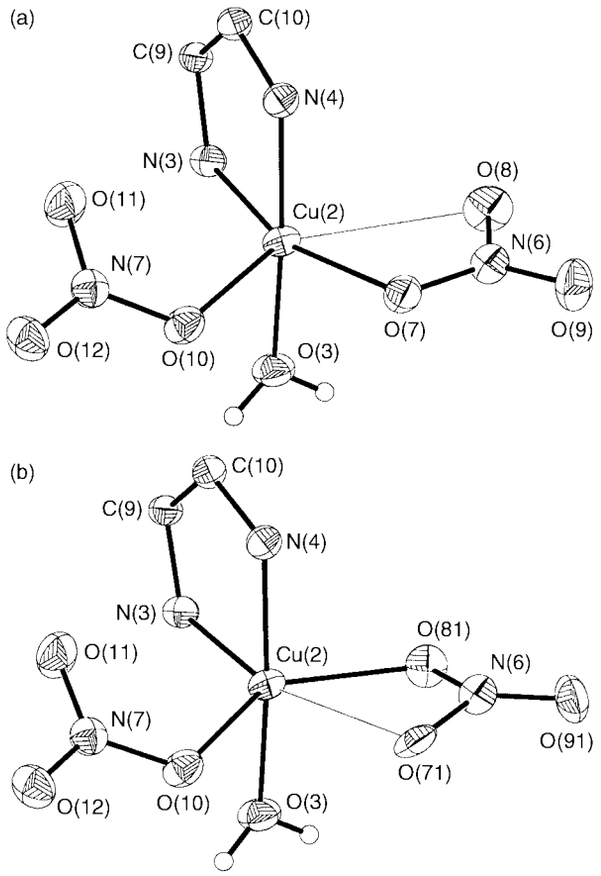

Fig. 5 Co-ordination spheres of Cu(2) in compound **3**: (a) major site of nitrate, (b) minor site of nitrate.

0.089 Å from the mean pap plane. The Cu · · · Cu separation across the pap bridge is 6.808 Å

All of the water hydrogen atoms participate in hydrogen bonding, linking the molecules in a three dimensional network. The molecules involved in the shortest intermolecular metal–metal distance, Cu(2) · · · Cu(1) ($\frac{3}{2} - x, -\frac{1}{2} + y, \frac{1}{2} - z$) of 5.504 Å, are linked by a medium strength hydrogen bond between water molecules in the respective co-ordination spheres. Both the major and the minor sites of the disordered nitrate participate in a hydrogen bond to water O(2) of a neighbour molecule. The relatively strong hydrogen bond between co-ordinated water and unco-ordinated nitrate, O(1)–H(10) · · · O(15), O · · · O being 2.640(3) Å is indicated in Fig. 4.

The major and minor sites of the disordered co-ordinated nitrate ion are related by an approximately 20° rotation around an axis running through N(6) and normal to the nitrate mean plane. The standard deviations in bond parameters of the minor site are three to four times larger than for the major site. The co-ordinated nitrate ions deviate significantly from three-fold symmetry, the strongly co-ordinated oxygen [O(4), O(7) (major site) and O(10)] in each case being associated with the longest N–O bond distance, and the angle opposite to this bond being the largest one. The unco-ordinated nitrate shows analogous features; here the longest N–O bond is associated with the oxygen atom participating in the relatively strong hydrogen bond mentioned above.

The bridging pap ligand. As there are no previous crystallographic reports on pap, free or as ligand, we would like to add a few comments as to the features observed in the present structures. In all three complexes the pap groups are essentially planar. Deviation from planarity is slightly more pronounced in the nitrate compound, where the accommodation of co-ordinated and semi-co-ordinated nitrate in the co-ordination spheres of copper apparently puts some extra strain on the bridging ligand. The *endo*-chelate C–N bonds fall in the range 1.352–1.369 Å and are significantly longer than the *exo*-chelate C–N bonds, being in the range 1.324–1.339 Å. The variation in the C–C bond lengths also follows a consistent pattern in the three compounds. In the central phenyl ring bonds are alternatingly long and short, the bonds shared between phenyl/pyrazine and phenyl/pyridyl being the shorter ones; in each case the C(4)–C(11)/C(4a) of the phenanthroline moiety is the longest bond, 1.466–1.469 Å.

Infrared and ESR spectra

No analysis of the infrared spectrum of pap has been published, but for pyridyl and pyrazine derivatives in general the ring vibrations are found in the region 1650–1300 cm^{-1}.[16a,b] Free pap shows a number of strong to medium absorption bands in this region: 1647 (br)s, 1590s, 1527m, 1481s, 1419s and 1392s cm^{-1}. Wide portions of this region are obscured in the spectra of complexes **1** and **3** due to the occurrence of strong absorptions for oxalate and nitrate, while in the spectrum of **2**, where the absorptions of the anion are out of this region, one can observe a pattern which is similar to that of free pap. For all three compounds **1**–**3** it is found that the aromatic ring vibrations in the region 1550 to 1450 cm^{-1} are shifted to higher wavenumbers on complex formation. This is consistent with metal co-ordination of the nitrogen atoms of the aromatic rings.[16c] Bands due to pap in the 1450 to 1370 cm^{-1} region can only be observed in the sulfate (**2**) and seem to be only marginally affected by metal complexation. For **1** strong bands centred around 1680, 1390 and 1260 cm^{-1} are consistent with bidentate oxalate co-ordination.[16d] A broad and very strong band centred around 1128 cm^{-1} and a strong band at 616 cm^{-1} show the presence of sulfate in **2**. The splitting of these bands for unidentate sulfate cannot be observed in this case, probably due to overlap of absorptions from both free and co-ordinated sulfate. A band of medium intensity at 969 cm^{-1} is a signature of unidentate sulfate.[16d] The presence of nitrate in **3** is evidenced by a broad feature centred around 1390 cm^{-1} and peaks at 825, 807 and 725 cm^{-1} as well as the combination band at 1760 cm^{-1}. The splitting of the band in the 800 to 830 cm^{-1} region is consistent with the presence of both co-ordinated and unco-ordinated nitrate.[15,16d]

The X-band ESR spectra of complexes **1**–**3** were recorded in the temperature range 4.2–290 K. Those of **1** and **2** appear as axial doublets with $g_{\|} = 2.26$ (**1**) and 2.32 (**2**) and $g_{\perp} = 2.07$ (**1**) and 2.09 (**2**) in the whole temperature range investigated. The intensity of the signals increases when cooling, but their shape does not vary. The sequence $g_{\|} > g_{\perp} > 2.0$ for both complexes clearly indicates a copper(II) $d_{x^2-y^2}$ ground state as confirmed by the structures (copper(II) ions in elongated CuN_2O_4 environments). In the case of complex **3** the occurrence of two quite different copper ions in the dinuclear entity, one (Cu(1)) being square pyramidal and the other (Cu(2)) being described as a mixture of square pyramidal and trigonal bipyramidal, accounts for the complexity of its ESR spectrum which appears as the sum of two axial doublets, two peaks at 3030 and 3080 G and two minima at 3180 and 3280 G. The shape of the spectrum does not vary with the temperature, but its intensity increases when cooling from 290 to 4 K, especially for the first maximum and the last minimum. A tentative assignment of these features leads to $g_1 = 2.23$, $g_2 = 2.19$, $g_3 = 2.12$ and $g_4 = 2.06$, where g_2 and g_4 should correspond to the parallel and perpendicular components of the $d_{x^2-y^2}$ copper magnetic orbital (Cu(1)) and g_1 and g_3 to the perpendicular and parallel components of a mainly d_{z^2} copper(II) magnetic orbital (Cu(2)). No evidence for magnetic coupling in **1**–**3** is observed in their ESR spectra, indicating that the exchange interaction between copper(II) ions through bridging pap in this series of complexes is very small, in agreement with the magnetic susceptibility measurements (see below).

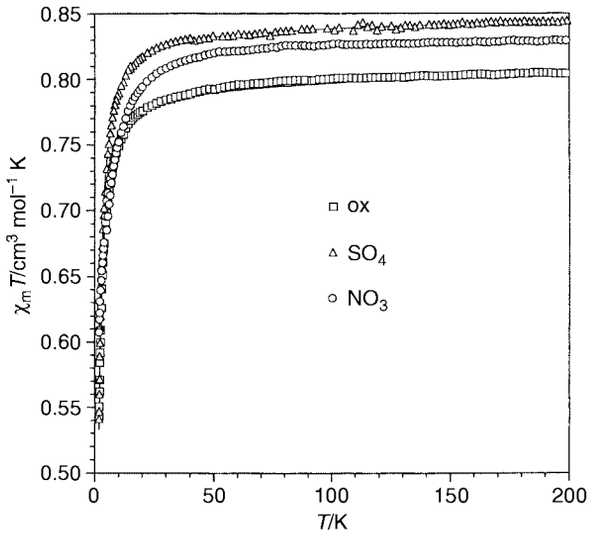

Fig. 6 Thermal dependence of $\chi_m T$ for complexes **1** (□), **2** (△) and **3** (○); solid line, best fit (see text).

Magnetic properties

The magnetic properties of complexes **1**–**3** are shown in Fig. 6 in the form of $\chi_m T$ *versus* T plots. The value of $\chi_m T$ at room temperature is 0.81 $cm^3\ mol^{-1}$ K for **1** and 0.84 $cm^3\ mol^{-1}$ K for **2** and **3**. These values are as expected for two magnetically isolated spin doublets. They remain practically constant when cooling and decrease sharply for $T < 20$ K attaining values of 0.54 (**1** and **2**) and 0.61 $cm^3\ mol^{-1}$ K (**3**) at 1.9 K. No susceptibility maximum is observed in the whole temperature range explored. These magnetic curves are indicative of Curie law behaviour with a very weak antiferromagnetic interaction. Taking into account the dinuclear nature of these complexes, we have used a simple Bleaney–Bowers expression to analyse their magnetic data,[17] the Hamiltonian being $H = J\ S_1 \cdot S_2$ (J is the singlet–triplet energy gap). The values of the relevant magnetic parameters obtained by least-squares fit through this expression are: $J = -1.4\ cm^{-1}$, $g = 2.06$ and $R = 1.7 \times 10^{-5}$ for **1**, $J = -1.5\ cm^{-1}$, $g = 2.10$ and $R = 4.5 \times 10^{-6}$ for **2** and $J = -1.3\ cm^{-1}$, $g = 2.08$ and $R = 6.0 \times 10^{-5}$ for **3**; R is the agreement factor defined as $\Sigma_i[(\chi_m T)_{obs(i)} - (\chi_m T)_{calc(i)}]^2/\Sigma_i[(\chi_m T)_{obs(i)}]^2$.

Our data reveal that magnetic interaction between the copper(II) ions separated by more than 6.7 Å through the pap bridge is very weak. To our knowledge, this is the first magnetostructural study dealing with the pap ligand and consequently no comparison can be made. From the molecular structures one can conclude that the unpaired electron on each metal centre in complexes **1** and **2** is clearly described by a $d_{x^2-y^2}$ magnetic orbital which is coplanar with the pap skeleton (the x and y axes being roughly defined by the copper to nitrogen bonds); in **3** the magnetic orbital of Cu(1) also has the same characteristics, while the distorted co-ordination geometry of Cu(2) will give the magnetic orbital some d_{z^2} character. The orientation of the magnetic orbitals in **1** and **2** is most favourable for magnetic coupling through the σ pathway, but the observed antiferromagnetic coupling is very weak, showing that the pap ligand does not efficiently propagate exchange by this mechanism. This result contrasts with the remarkable efficiency of 2,2′-bipyrimidine to transmit magnetic interaction.[4] In both cases the σ pathway is involved, but the presence of one additional carbon atom in the bridging skeleton in the case of pap (Cu–N–C–C–N–Cu′ for pap *versus* Cu–N–C–N–Cu′ for bpm) seems to play a major role in its ability to transmit electronic interactions. The total Cu···Cu separation in the present compounds should not in itself preclude magnetic interaction. In *e.g.* hydranilato-bridged complexes, where the Cu···Cu separation is around 7.6 Å, significant antiferromagnetic interaction is encountered (J around $-20\ cm^{-1}$).[18] Even so, when comparing hydranilato- and oxalato-bridged complexes we see that the addition of extra carbon atoms in the bridging skeleton (O–C–C–C–O in anilate *versus* O–C–O in oxalate) is accompanied by a large reduction in the exchange parameter for comparable co-ordination geometries.[19] Looking at the pyrazine-bridging fragment of pap, it seems appropriate to make a comparison with the magnetostructurally characterized pyrazine-bridged copper(II) complexes.[5] The magnetic couplings in several of these compounds are significantly stronger than those observed through pap in the present work. As the geometries of most pyrazine-bridged complexes leave both the σ and the π pathways available, the interpretation of these results is not obvious. However, assuming that a σ superexchange mechanism is operative in pyrazine, the weaker interaction through pap may be related to the greater electronic delocalization of pap as compared to pyrazine. This may cause a stabilization of the HOMOs of pap and hence increase the energy difference to the magnetic copper d orbital, leading to less mixing of these orbitals and a weaker magnetic interaction. The debate on whether σ or π pathways are operative in pyrazine complexes is still alive.[5h,i,6] In this context it must be mentioned that in two copper(II) tetra(2-pyridyl)pyrazine compounds, which are the only pyrazine-bridged copper(II) complexes so far found to have strong antiferromagnetic interaction, the copper co-ordination geometries are compatible with a σ pathway.[6] It is to be noted that the Cu–$N_{pyrazine}$ bonds are particularly short in the tetra(2-pyridyl)pyrazine complexes, 1.957–1.976 Å, as compared to the range 2.011–2.062 Å found in the pap-bridged compounds presented in this work. Further magnetostructural studies to check out the efficiency of the π pathway through the pap ligand are planned. Work aimed at obtaining and structurally characterizing framework polynuclear metal complexes of this ligand is in progress, and a further goal is to investigate the possibility of spin crossover in such compounds.

Acknowledgements

The gift of 4,7-phenanthroline-5,6-dione from Novartis Norge AS is greatly appreciated. X-Ray equipment used in this investigation was financed through grants from the Research Council of Norway and the University of Bergen. M. J. and F. L. acknowledge financial support from the Spanish Dirección General de Investigación Científica y Técnica through project PB97-1397. Thanks are due to Dr Luis Lezama for recording the ESR spectra.

References

1 (*a*) P. Schmidt and J. Druey, *Helv. Chim. Acta*, 1957, **40**, 350; (*b*) S. Imor, R. J. Morgan, S. Wang, O. Morgan and A. D. Baker, *Synth. Commun.*, 1996, **26**, 2197.
2 B. J. Yoblinski, M. Stathis and T. F. Guarr, *Inorg. Chem.*, 1992, **31**, 5; Y. Fuchs, S. Lofters, T. Dieter, W. Shi, R. Morgan, T. C. Strekas, H. D. Gafney and A. D. Baker, *J. Am. Chem. Soc.*, 1987, **109**, 2691; L. DeCola and F. Barigelletti, *Gazz. Chim. Ital.*, 1988, **118**, 417.
3 R. J. Morgan, S. Chatterjee, A. D. Baker and T. C. Strekas, *Inorg. Chem.*, 1991, **30**, 2687; T. C. Strekas, A. D. Baker, O. Harripersad-Morgan and R. J. Morgan, *J. Coord. Chem.*, 1995, **34**, 77 and references therein.
4 I. Castro, J. Sletten, L. K. Glærum, F. Lloret, J. Faus and M. Julve, *J. Chem. Soc., Dalton Trans.*, 1994, 2777; I. Castro, J. Sletten, L. K. Glærum, J. Cano, F. Lloret, J. Faus and M. Julve, *J. Chem. Soc., Dalton Trans.*, 1995, 3207; M. Julve, G. De Munno, G. Bruno and M. Verdaguer, *Inorg. Chem.*, 1988, **27**, 3160.
5 (*a*) D. B. Losee, H. W. Richardson and W. E. Hatfield, *J. Chem. Phys.*, 1973, **59**, 3600; (*b*) H. W. Richardson and W. E. Hatfield, *J. Am. Chem. Soc.*, 1976, **98**, 835; (*c*) H. W. Richardson, J. R. Wasson and W. E. Hatfield, *Inorg. Chem.*, 1977, **16**, 484; (*d*) A. B. Blake and W. E. Hatfield, *J. Chem. Soc., Dalton Trans.*, 1978, 869; (*e*) M. S. Haddad, D. N. Hendrickson, J. P. Cannady, R. S. Drago and D. S. Bieksza, *J. Am. Chem. Soc.*, 1979, **101**, 898; (*f*) J. Darriet, M. S. Haddad, E. N. Duesler and D. N. Hendrickson, *Inorg. Chem.*,

1979, **18**, 2679; (*g*) M. Julve, M. Verdaguer, J. Faus, F. Tinti, J. Moratal, A. Monge and E. Gutiérrez-Puebla, *Inorg. Chem.*, 1987, **26**, 3520; (*h*) H. Oshio and U. Nagashima, *Inorg. Chem.*, 1990, **29**, 2231; (*i*) J. Suárez-Varela, E. Colacio, A. Romerosa, J. C. Avila-Rosón, M. A. Hidalgo and J. Romero, *Inorg. Chim. Acta*, 1994, **217**, 39.
6 M. Graf, H. Stoeckli-Evans, A. Escuer and R. Vicente, *Inorg. Chim. Acta*, 1997, **257**, 89; M. Graf, B. Greaves and H. Stoeckli-Evans, *Inorg. Chim. Acta*, 1993, **204**, 239.
7 J. Sletten and O. Bjørsvik, *Acta Chem. Scand.*, 1998, **52**, 770; H. Grove and J. Sletten, unpublished work.
8 J. Unterzaucher, *Mikrochem. Ver. Mikrochim. Acta*, 1951, **36/37**, 706.
9 A. Earnshaw, in *Introduction to Magnetochemistry*, Academic Press, London, 1968.
10 G. M. Sheldrick, SADABS, Empirical Absorption Correction Program, University of Göttingen, 1996.
11 SMART, Version 4.0, Data Collection Software; SAINT, Version 4.0, Data Integration Software, Bruker AXS, Inc., Madison, WI, 1997.
12 G. M. Sheldrick, *Acta Crystallogr.*, *Sect. A*, 1990, **46**, 467; G. M. Sheldrick, SHELXL 93, University of Göttingen, 1993; XP, Version 4.3, Siemens Analytical X-Ray Instrument Inc., Madison, WI, 1992.
13 (*a*) I. M. Procter, B. J. Hathaway and P. Nicholls, *J. Chem. Soc. A*, 1968, 1678; (*b*) B. J. Hathaway, *Struct. Bonding* (*Berlin*), 1984, **57**, 55.
14 A. W. Addison, T. Nageswara Rao, J. Reedijk, J. van Rijn and G. C. Verschoor, *J. Chem. Soc.*, *Dalton Trans.*, 1984, 1349.
15 C. C. Addison, N. Logan, S. C. Wallwork and C. D. Garner, *Q. Rev. Chem. Soc.*, 1971, **25**, 289.
16 (*a*) J. R. Allan and A. D. Paton, *Thermochim. Acta*, 1993, **214**, 227; (*b*) J. G. H. Du Preez, T. I. A. Gerber and R. Jacobs, *J. Coord. Chem.*, 1994, **33**, 147; (*c*) J. R. Allan, N. D. Baird and A. L. Kassyk, *J. Therm. Anal.*, 1979, **16**, 79; (*d*) K. Nakamoto, in *Infrared and Raman Spectra of Inorganic and Coordination Compounds*, 3rd edn., Wiley, New York, 1978.
17 B. Bleaney and K. D. Bowers, *Proc. R. Soc. London*, *Ser. A*, 1952, **214**, 451.
18 F. Tinti, M. Verdaguer, O. Kahn and J.-M. Savariault, *Inorg. Chem.*, 1987, **26**, 2380.
19 M. Julve, M. Verdaguer, A. Gleizes, M. Philoche-Levisalles and O. Kahn, *Inorg. Chem.*, 1984, **23**, 3808.

Paper a907658a